

# Attractor reconstruction with reservoir computers: The effect of the reservoir's conditional Lyapunov exponents on faithful attractor reconstruction

Joseph D. Hart

January 3, 2024

## Abstract

Reservoir computing is a machine learning technique which has been shown to be able to replicate the chaotic attractor, including the fractal dimension and the entire Lyapunov spectrum, of the dynamical system on which it is trained. We quantitatively relate the generalized synchronization dynamics of a driven reservoir computer during the training stage to the performance of the autonomous reservoir computer at the attractor reconstruction task. We show that, for successful attractor reconstruction and Lyapunov exponent estimation, the largest conditional Lyapunov exponent of the driven reservoir must be significantly smaller (more negative) than the smallest (most negative) Lyapunov exponent of the true system. We find that the maximal conditional Lyapunov exponent of the reservoir depends strongly on the spectral radius of the reservoir adjacency matrix, and therefore, for attractor reconstruction and Lyapunov exponent estimation, small spectral radius reservoir computers perform better in general. Our arguments are supported by numerical examples on well-known chaotic systems.

## 1 Introduction

A common problem encountered in many areas of science occurs when a model (or at least an estimation of the ergodic properties) of a dynamical system is required, but models based on first-principles are either unavailable, inaccurate, or intractable. In these cases, analysis must be developed based on time series data. Often, this is done by delay embedding techniques [1, 2]; however, machine learning approaches have recently shown significant promise in data-driven model development for dynamical systems [3]. Reservoir computing is one machine learning approach that has been shown to be particularly well suited for the analysis of dynamical systems [4, 5].

In particular, it has been shown that a well-trained reservoir computer, when operated as an autonomous feedback system, can replicate the attractor of the dynamical system on which it is trained, allowing it to not only produce accurate long-term prediction of chaotic time series (over five Lyapunov times [6]), but also to provide estimates of ergodic dynamical quantities such as the fractal dimension and entire Lyapunov spectrum of the true dynamical system [6, 7, 8]. Perhaps most impressive is that reservoir computers were shown to be capable of providing accurate estimates of the negative Lyapunov exponents of the true dynamical system using only time series data, which is known to be a particularly difficult problem for other data-based Lyapunov exponent estimation techniques [9, 10, 11, 1, 2]. Indeed, the reproduction of the Lyapunov spectrum has been suggested as a metric for evaluating a reservoir computer's performance at the attractor reconstruction task [8, 12]. While other metrics of attractor reconstruction, such as medium-term prediction error [13, 14], are also commonly used, in this work we use the Lyapunov spectrum metric.

Despite this promise of reservoir computing for attractor reconstruction and estimating Lyapunov exponents from time series, Pathak et al. were unable to reproduce the negative Lyapunov exponent (and, therefore, the attractor dimension) of the Lorenz system, even though their reservoir computer accurately reproduced the positive and zero exponents and otherwise appeared to provide an accurate attractor reconstruction [6]. Pathak et al. attributed this failure to the especially thin transverse structure of the Lorenz return map, a peculiarity of the Lorenz system.

In this work, we show that the cause of this failure of the reservoir computer to reproduce the negative Lyapunov exponents is general and can be attributed to the dynamics of the reservoir network itself. In the training phase, the reservoir network acts as a nonlinear filter driven by a chaotic signal, which is known to result in an increase in the fractal dimension when the filter conditional Lyapunov exponents are less negative than those of the drive system [15, 16]. We argue that the magnitude of the maximal reservoir conditional Lyapunov exponent is predictive of whether the trained autonomous reservoir computer can replicate the negative Lyapunov exponents and the fractal dimension of the true chaotic system: For successful Lyapunov spectrum replication, the maximal conditional Lyapunov exponent of the driven reservoir must be significantly more negative than the most negative Lyapunov exponent of the true system. In other words, the reservoir contraction to the generalized synchronization manifold must be significantly faster than the contractions experienced by the true dynamical system, otherwise the reservoir Lyapunov exponents will take the place of the true negative Lyapunov exponents in the Lyapunov spectrum. Our arguments are supported by numerical examples on well-known chaotic systems. We also find that the maximal conditional Lyapunov exponent of the reservoir depends strongly on the spectral radius of the reservoir adjacency matrix, suggesting that reservoirs with spectral radius significantly smaller than one are better suited in general to the attractor reconstruction task than reservoirs with spectral radius near or greater than one.

Our results not only provide insight into the key dynamical features that enable a reservoir computer to perform successful attractor reconstruction, but also provide an indicator for when one might expect that a trained reservoir computer has provided an accurate estimate of the negative Lyapunov exponents and attractor dimension of an unknown dynamical system.

## 2 Reservoir computing

A reservoir computer (RC) [17, 18] (here, we use an echo state network implementation [5]) is a type of recurrent neural network that is designed to be particularly easy to train. An RC consists of three layers: a linear input layer, a nonlinear recurrent layer (called the reservoir), and an output layer. Only the output layer is trained, allowing for computationally inexpensive training procedures such as ridge regression [19]. Reservoir computing has been shown to be well-suited to the performance of a variety of time-series analysis tasks, such as inferring unseen bifurcations, attractors, and tipping points [20, 21, 22, 23], causal inference [24, 25], chaos synchronization [26] and communication [27], and nonlinear control [28] in a wide range of dynamical systems including delay systems [21], spatio-temporal systems [6, 29, 21, 22] such as fluid turbulence [30] and atmospheric dynamics [31, 32], and real-world systems such as complex machinery [33] and networks of neurons [34].

Each RC used here consists of a recurrent neural network of  $N$  discrete-time nodes with random network topology (Erdős-Renyi random networks with average degree 6). Let  $\mathbf{r}[n]$  be an  $N \times 1$  column vector that describes the state of the reservoir at time  $n$ . During training, the reservoir operates as a driven nonlinear dynamical system described by

$$\mathbf{r}[n+1] = \tanh(A\mathbf{r}[n] + W^{in}\mathbf{x}[n] + \mathbf{b}), \quad (1)$$

where  $\mathbf{x}[n]$  is an  $\mathcal{D} \times 1$  column vector describing the input signal to the reservoir,  $W^{in}$  is an  $N \times \mathcal{D}$  matrix describing the input layer,  $A$  is an  $N \times N$  matrix describing the inter-nodal connections in the reservoir layer, and  $\mathbf{b}$  is an  $N \times 1$  bias vector with elements chosen randomly and uniformly between -1 and 1. In this work, we consider input signals that are created by sampling a continuous-time dynamical system described by the state vector  $\mathbf{x}(t)$ , such that  $\mathbf{x}[n] \equiv \mathbf{x}(n\tau)$  where  $\tau$  is the uniform sampling time.

For the task of attractor reconstruction, the reservoir is driven by the input signal  $\mathbf{x}[n]$  in the training phase. The reservoir state  $\mathbf{r}[n]$  is recorded at each time step after some initial transient time and the RC is trained to predict that signal at the next time step  $\mathbf{x}[n+1]$ ; this prediction  $\hat{\mathbf{x}}$  is obtained from the reservoir by

$$\hat{\mathbf{x}}[n] = W^{out}\mathbf{P}(\mathbf{r}[n]), \quad (2)$$

where  $\mathbf{P}$  is an  $N_p$ -dimensional function of  $\mathbf{r}$ , and  $W^{out}$  is a  $\mathcal{D} \times N_p$  matrix obtained by ridge regression [19]. Often, the choice  $P(\mathbf{x}) = \mathbf{x}$  is made.

Once the training is complete, attractor reconstruction can be attempted by feeding the prediction  $\hat{\mathbf{x}}$  back into the reservoir as the input, turning the reservoir into an autonomous dynamical system:

$$\mathbf{r}[n+1] = \tanh(A\mathbf{r}[n] + W^{in}\hat{\mathbf{x}}[n] + \mathbf{b}). \quad (3)$$

Attractor reconstruction does not always succeed, even when the one-step-ahead training error is very small. Often, when attractor reconstruction fails, the RC approaches an untrained attractor, such as a fixed point or a limit cycle [35].

When attractor reconstruction does succeed it has been shown that the autonomous RC described by Eq. 3 can provide a stable reconstruction of the attractor of a dynamical system as quantified by density distributions, Poincaré sections, Lyapunov exponents, and information dimension [6, 35, 7]. However, it is known that in some cases, even though the density distributions and Poincaré sections of the RC output and the true system are essentially indistinguishable, the negative Lyapunov exponents (and therefore the Kaplan-Yorke dimension) of the true system are not reproduced by the autonomous reservoir, while in other cases a large number of the true system negative Lyapunov exponents are reproduced with remarkable accuracy [6]. In this work, we shed some light on when RCs fail to reproduce the true negative Lyapunov exponents, and we discuss how one can tune a RC to be more likely to reproduce the true negative Lyapunov exponents and therefore the true Kaplan-Yorke dimension.

## 2.1 Generalized synchronization and reservoir computing

Generalized synchronization between two dynamical systems (often a drive system and a response system) occurs when there is a functional relationship between the dynamical variables of the two systems [36, 37, 38]. A standard test for generalized synchronization is the auxiliary system approach [38]: Two identical copies of the response system with different initial conditions synchronize with each other when driven by the same drive signal if and only if they display generalized synchronization with the drive signal. The rate at which the two response systems from the auxiliary system converge to the same trajectory can be quantified by the conditional Lyapunov exponents (CLEs) [39]. Generalized synchronization is stable if and only if all CLEs are negative [38, 37].

Generalized synchronization and the closely related concept of consistency [40] of the reservoir response to the drive signal have been identified as essential for a RC to be effective and reliable [35, 41, 42, 43, 44, 45, 46, 47, 8, 12]. Despite this extensive literature, only a few works have considered the impact of the magnitude of the reservoir's maximal CLE on any type of reservoir computing task [47, 41, 8]. As far as we are aware, none have linked the magnitude of the maximal CLE of the reservoir to the reservoir's performance at the attractor reconstruction task, as we do in the following sections.

## 2.2 Conditional Lyapunov exponents and attractor reconstruction

It is well-established that an increase in dimension can occur in filtered dynamical signals [15]. In order to understand this, we recall the Kaplan-Yorke conjecture [48]: the information dimension of a dynamical system is given by  $\mathcal{D}_{KL} = j + \lambda_j/|\lambda_{j+1}|$ , where  $j$  is the largest index for which the sum  $\sum_{k=1}^j \lambda_k$  is non-negative. A stable linear filter will have negative Lyapunov exponents; however, if the filter Lyapunov exponents are larger than the negative exponents of the driving chaotic system, the filter Lyapunov exponents can replace some of the driving system Lyapunov exponents in the summation used to calculate the Kaplan-Yorke dimension. In such a case, the filtered dynamical system will have a different dimension from the driving dynamical system, sometimes substantially so [15, 16, 49]. For example, if the driving system is the Lorenz system with the standard parameters (Eq. 4 below) and the filter is stable (maximal Lyapunov exponent of the filter  $\lambda_{max}^{(filter)} < 0$ ), then the three largest LEs of the filtered chaotic system are  $\lambda_1^{(Lorenz)}$ ,  $\lambda_2^{(Lorenz)}$ , and  $\max(\lambda_3^{(Lorenz)}, \lambda_{max}^{(filter)})$ , and so the dimension of the filtered chaotic system depends on  $\lambda_{max}^{(filter)}$ .

This argument also holds for nonlinear filters [15]. The driven (non-autonomous) reservoir can be thought of as a nonlinear filter. Unlike the case of linear filters, for nonlinear filters the filter Lyapunov exponents depend on the drive signal itself, and are therefore called conditional Lyapunov exponents (CLEs) [39]. A reservoir has  $N$  CLEs, while the complete reservoir-and-drive system (considered as a whole) has  $N + \mathcal{D}$  Lyapunov exponents.

For the tasks of attractor reconstruction and Lyapunov exponent estimation, the RC is operated in autonomous mode, in which the RC output is fed back and used as the input to the reservoir. Thus, there is no concept of CLEs, and there are  $N$  total Lyapunov exponents.

Nevertheless, when attractor reconstruction is successful, the RC output is a good approximation of the true driving system [6, 35]. In this case, one might expect the reservoir to replicate the true Lyapunov exponents while the other Lyapunov exponents of the autonomous RC stay close to the CLEs of the driven, non-autonomous reservoir. We find that this is often the case. We therefore use the maximal CLE of the reservoir as an estimate of the maximal Lyapunov exponent that should be attributed to the RC itself rather than to the true dynamical system.

For successful attractor reconstruction, the RC should replicate the ergodic properties of the dynamical system on which it is trained, including the Lyapunov exponents and the information dimension. According to the arguments above, this is possible only if the reservoir CLEs are more negative than the most negative Lyapunov exponent of the true dynamical system. As shown below, we find the best performance when the reservoir CLEs are significantly more negative than the true negative exponents.

We note that even when attractor reconstruction does succeed and the reconstructed attractor is locally stable, the autonomous RC can exhibit multistability in which untrained attractors can be reached from certain initial conditions [14, 50]. In this work, we assume that the RCs are on the trained attractor. Since the CLE and LE spectra are properties of a specific attractor, we do not expect the potential presence of multiple attractors to affect these quantities.

Much attention is paid to the spectral radius of the reservoir. Conventional wisdom is that the spectral radius of the RC should be near 1 [4, 51], as this is thought to provide a good trade off between long memory and stability (generalized synchronization). However, “memory” in terms of reservoir computing is often considered to be the inverse of the maximal CLE: a larger maximal CLE leads to greater memory [49]. According to the arguments above, this “memory” can apparently be detrimental for the task of attractor reconstruction (defined as successful when the Lyapunov exponents and dimension of the trained autonomous RC agrees with the true Lyapunov exponents and attractor dimension), and the reservoir spectral radius should often be significantly lower than 1 for this task, as was noted in Ref. [52]. Other definitions of successful attractor reconstruction, such as accurate short- or medium-term prediction error, can result in different optimal values for the reservoir spectral radius [13, 14, 50].

In the following sections, we provide evidence for these arguments by performing attractor reconstruction on the Lorenz and Qi chaotic systems using RCs with a variety of different spectral radii. We find that the autonomous RC replicates the Lyapunov spectra and Kaplan-Yorke dimension of the true dynamical system only when the maximal CLE is sufficiently small and that the maximal CLE is strongly correlated with the spectral radius.

### 3 Results: Lorenz system

#### 3.1 The Lorenz Equations

The Lorenz system is described by [53]

$$\begin{aligned} \frac{dx}{dt} &= \sigma(y - x) + a\xi_x(t) \\ \frac{dy}{dt} &= x(\rho - z) - y + a\xi_y(t) \\ \frac{dz}{dt} &= xy - \beta z + a\xi_z(t) \end{aligned} \quad (4)$$

with  $\sigma = 10$ ,  $\beta = 8/3$  and  $\rho = 28$  or  $\sigma = 20$ ,  $\beta = 4$ , and  $\rho = 45.92$ . The first set of parameters is the standard set; the second has been shown to have a large magnitude negative Lyapunov exponent [54]. The intrinsic noise  $\xi(t)$  is Gaussian white noise with unit standard deviation and the different  $\xi_i$  are independent. We choose the intrinsic noise strength  $a = 0.01$ ; intrinsic noise is known to help with the RC training in some cases [24, 55, 25]. The equations were numerically integrated using a second order Runge-Kutta with the noise handled in the method of Honeycutt [56] with an integration time step of 0.001. The time series obtained by the integration were downsampled to have  $\tau = 0.02$ , as in [6, 52]. All three variables of the Lorenz system are used as inputs to the reservoir.

We consider two different values for the Lorenz parameters. We compute the true Lyapunov spectra to be 0.91, 0.0, -14.6 ( $\sigma = 10$ ) and 1.5, 0.0, and -26.5 ( $\sigma = 20$ ) in agreement with [6, 54].

### 3.2 Attractor reconstruction

For each value of the reservoir spectral radius, we create, train, and test 1000 RCs with  $N = 300$  nodes. Following Ref. [6], the reservoir output  $\hat{\mathbf{x}} = [\hat{x}, \hat{y}, \hat{z}]$  is given by

$$\begin{bmatrix} \hat{x}[n] \\ \hat{y}[n] \\ \hat{z}[n] \end{bmatrix} = W^{out} \begin{bmatrix} \mathbf{r}[n] \\ \mathbf{r}[n] \\ \tilde{\mathbf{r}}[n] \end{bmatrix}, \quad (5)$$

where  $\tilde{\mathbf{r}}$  is defined such that the first half of its elements are the same as that of  $\mathbf{r}$ , while  $\tilde{\mathbf{r}} = r^2$  for the remaining half of the reservoir nodes. The RCs differ in their input strengths  $\sigma_{in}$  (chosen randomly in the range  $(0, 0.2]$ ), random network topologies, and bias vectors. We use 40000 training time steps and set the ridge regression parameter  $\beta = 0$  for the training (so that only simple regression is used); the noise is sufficient to prevent overfitting [57, 58]. The ten “best” attractor reconstructions are retained, where the attractor reconstructions are ranked according to the mean square error between the power spectra of the reconstructed  $x$  variable and of the true  $x$  variable, computed over 20000 time steps. The Lyapunov spectra of the trained, autonomous RCs are computed using 100000 time steps. Additionally, the CLE spectra of the driven reservoirs are computed over the 40000 training time steps for these retained reservoirs.

First, we consider the attractor reconstruction task on the Lorenz system with the traditional parameters. The results are shown in Fig. 1. Figure 1(a) shows the three largest Lyapunov exponents of the autonomous RC plotted as a function of the maximal reservoir CLE. The Lyapunov exponents of the true Lorenz system are shown as horizontal gray lines. The agreement between the first two Lyapunov exponents of the autonomous RC Lyapunov exponents and the true system Lyapunov exponents is excellent in all cases. For the third Lyapunov exponent (purple triangles), the agreement is excellent for very negative maximal CLE. However, as the maximal CLE increases and approaches the negative LE of the true system, the disagreement increases significantly. The reason for this disagreement is described in Section 2.2: Once the reservoir CLEs have increased such that they are greater than the negative LE of the true system, the reservoir dynamics are now too slow to capture the negative LE of the true system, and the maximal CLE of the reservoir replaces the negative LE of the true system as the third-largest LE of the autonomous RC. Evidence for this is provided by the fact that the  $\lambda_3$  mostly lie along the curve  $\lambda = \max(\lambda_3^{(Lorenz)}, \max(CLE))$ , as predicted in Section 2.2.

Figure 1(b) shows that the maximal CLE is strongly correlated with spectral radius. Variations for a fixed spectral radius are due to the different input strengths and reservoir network topologies. For confirmation, Fig. 1(c) shows the reservoir Lyapunov exponents as a function of the reservoir spectral radius; one sees that the Lyapunov exponent estimation becomes unreliable for spectral radii greater than about 0.8. The large spread in  $\lambda_3$  for larger values of spectral radius is due to the fact that, at these values of spectral radius,  $\lambda_3$  is determined by the maximal CLE and the maximal CLE is not fully determined by (only strongly correlated with) the spectral radius.

We note that we believe that this effect is likely the reason that previous efforts [6] at attractor reconstruction using a large reservoir spectral radius have been unsuccessful at replicating the negative Lyapunov exponent of the Lorenz system.

We now consider the attractor reconstruction task on the Lorenz system with the modified parameters. The results are shown in Fig. 2, and are very similar to the case of the traditional Lorenz parameters. Figure 2(a) shows the three largest Lyapunov exponents of the autonomous reservoir computer plotted as a function of the maximal CLE of the driven reservoir. The Lyapunov exponents of the true Lorenz system are shown as horizontal gray lines. The agreement between the first two Lyapunov exponents of the autonomous RC and the true system Lyapunov exponents is excellent in all cases. For the third Lyapunov exponent (purple triangles), the agreement is excellent for very negative maximal CLE. However, as the maximal CLE increases, the disagreement increases significantly. The reason for this disagreement is described in Section 2.2: Once the reservoir CLEs have increased such that they are greater than the negative LE of the true system, the reservoir dynamics are now too slow to capture the negative LE of the true system, and the maximal CLE of the reservoir replaces the negative LE of the true system as the third-largest LE of the autonomous RC. Evidence for this is provided by the fact that the  $\lambda_3$  mostly lie along the curve  $\lambda = \max(\lambda_3^{(Lorenz)}, \max(CLE))$ , as predicted in Section 2.2.

There appear to be no deleterious effects of having a very negative maximal CLE, corresponding to a short reservoir memory, for this task. Figure 2(b) shows that the maximal CLE is strongly correlated

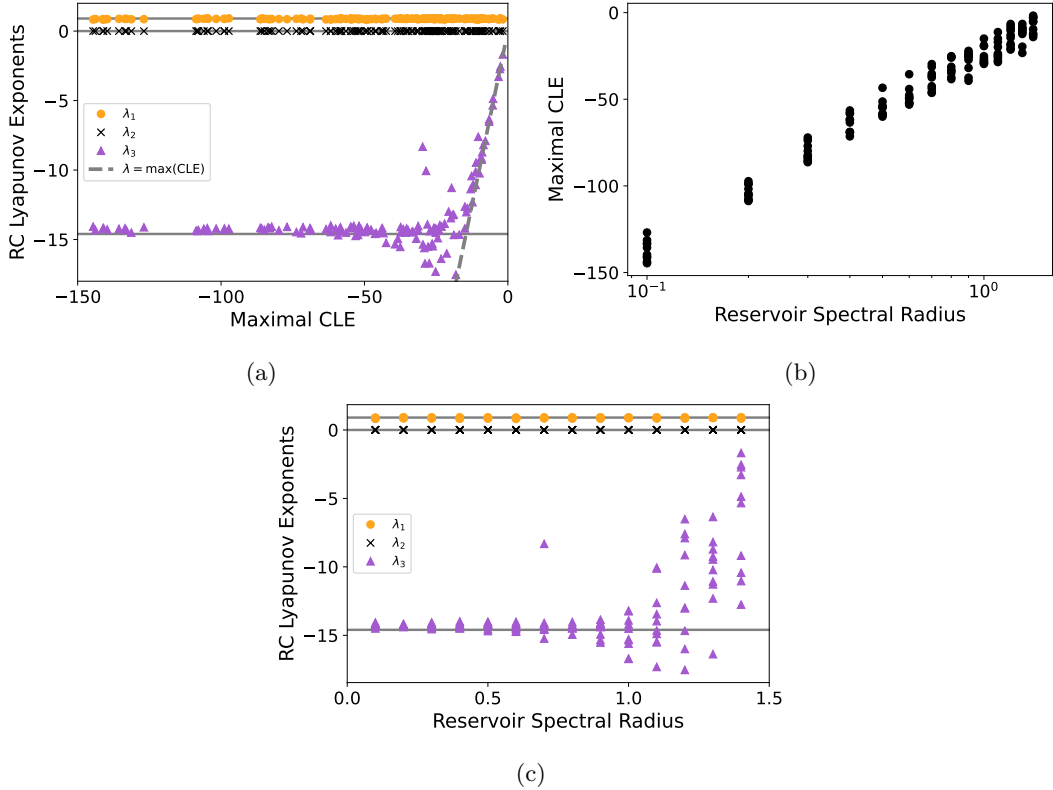


Figure 1: Lorenz system with standard parameters:  $\sigma = 10$ ,  $\beta = 8/3$  and  $\rho = 28$ . (a) Three largest Lyapunov exponents of the trained autonomous RC vs the maximal CLE of the driven RC before training. The Lyapunov exponents of the true system are indicated as solid gray lines. The line  $\lambda = \max(\text{CLE})$  is shown as a dashed gray line. (b) Maximal CLE of the driven reservoir vs the reservoir spectral radius. (c) Three largest Lyapunov exponents of the trained autonomous RC vs the reservoir spectral radius.

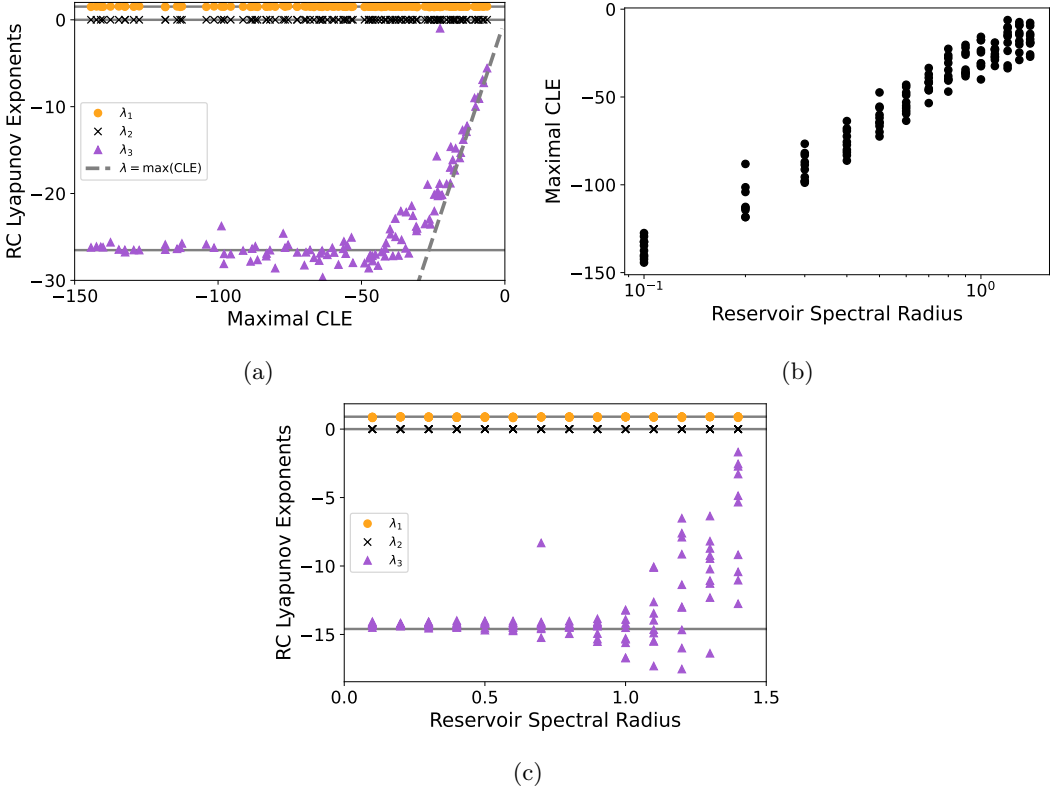


Figure 2: Lorenz system with  $\sigma = 20$ ,  $\beta = 4$ , and  $\rho = 45.92$ . (a) Three largest Lyapunov exponents of the trained autonomous RC vs the maximal CLE of the driven RC before training. The Lyapunov exponents of the true system are indicated as solid gray lines. The line  $\lambda = \max(\text{CLE})$  is shown as a dashed gray line. (b) Maximal CLE of the driven reservoir vs the reservoir spectral radius. (c) Three largest Lyapunov exponents of the trained autonomous RC vs the reservoir spectral radius.

with spectral radius. Variations for a fixed spectral radius are due to the different input strengths and reservoir network topologies.

Figure 2(c) shows the Lyapunov exponents of the autonomous RC as a function of the reservoir spectral radius; one sees that the Lyapunov exponent estimation becomes unreliable for spectral radii greater than about 0.7. The difference in the threshold spectral radii is due to the difference in negative Lyapunov exponent in the two different Lorenz parameter sets. The large spread in  $\lambda_3$  for larger values of spectral radius is due to the fact that, at these values of spectral radius,  $\lambda_3$  is determined by the maximal CLE and the maximal CLE is not fully determined by (only strongly correlated with) the spectral radius.

We now consider the effect of the maximal CLE of the driven reservoir (or the reservoir spectral radius) on the Kaplan-Yorke dimension of the autonomous RC, shown in Fig. 3. As the maximal CLE nears and surpasses the negative Lorenz Lyapunov exponent, the Kaplan-Yorke dimension increases, as expected [15]. Therefore, we find that a large reservoir spectral radius (large reservoir maximal CLE) results in poor attractor reconstruction, as quantified by replication of the entire true Lyapunov spectrum.

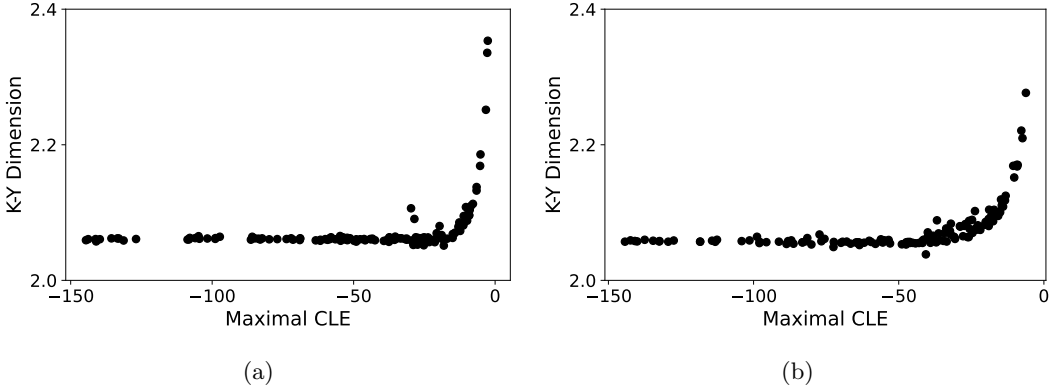


Figure 3: Kaplan-Yorke dimension of the trained autonomous RC vs maximal CLE of the driven reservoir before training for the Lorenz system with (a)  $\sigma = 10$ ,  $\beta = 8/3$  and  $\rho = 28$  and (b)  $\sigma = 20$ ,  $\beta = 4$ , and  $\rho = 45.92$ . In both cases, the Kaplan-Yorke dimension of the RC increases sharply as the maximal CLE of the reservoir approaches zero (i.e., as  $\rho$  increases), indicating that the autonomous RC does not accurately replicate the Lorenz attractor geometry  $\rho$  greater than about 0.8.

## 4 Results: A four-dimensional chaotic system

### 4.1 The Qi Equations

The Qi system [59] is a well-characterized four-dimensional chaotic system with a butterfly attractor. The Qi system is described by

$$\begin{aligned} \frac{dx_1}{dt} &= p_1(x_2 - x_1) + x_2 x_3 x_4 + a \xi_1(t) \\ \frac{dx_2}{dt} &= p_2(x_1 + x_2) + x_1 x_3 x_4 + a \xi_2(t) \\ \frac{dx_3}{dt} &= -p_3 x_3 + x_1 x_2 x_4 + a \xi_3(t) \\ \frac{dx_4}{dt} &= -p_4 x_4 + x_1 x_2 x_3 + a \xi_4(t). \end{aligned} \quad (6)$$

As with the Lorenz system, we choose a noise strength  $a = 0.01$ . In this work, we choose  $p_1 = 35$ ,  $p_2 = 10$ ,  $p_3 = 1$  and  $p_4 = 10$  since these parameter values are known to result in a chaotic system with one positive Lyapunov exponent, and two well-separated negative Lyapunov exponents (along with a zero exponent) [59]. For these parameters, we compute a Lyapunov spectrum of 3.26, 0.00, -4.14, and -35.12. These well-separated negative Lyapunov exponents create a more strenuous test of our hypothesis that the maximal CLE of the reservoir network (which is strongly dependent on the reservoir spectral radius) places a limitation on the minimum Lyapunov exponent that the autonomous RC can display.

The intrinsic noise  $\xi(t)$  is Gaussian white noise with unit standard deviation and the different  $\xi_i$  are independent. We choose the intrinsic noise strength  $a = 0.01$ ; intrinsic noise is known to help with the RC training in some cases [24, 55, 25]. To generate the training data, we integrate Eq. 6 using Honeycutt's second order Runge-Kutta method [56] with a time step of 0.0001. To obtain the RC input data, we downsample the time series so that  $\tau = 0.01$ . All four variables from the Qi system are used as inputs to the reservoir.

### 4.2 Lyapunov spectrum estimation

For each value of the reservoir spectral radius, we create, train, and test 1000 RCs with  $N = 400$  nodes and with  $\mathbf{P}(\mathbf{x}) = \mathbf{x}$ . We use 400 nodes. The RCs differ in their input strengths  $\sigma_{in}$  (chosen randomly in the range  $(0,1]$ ), network topologies (Erdos-Renyi random networks with average degree 6), and bias vectors (randomly chosen between -1 and 1). We use 40000 training time steps and a ridge regression parameter of  $10^{-8}$  is used. Again, the ten “best” attractor reconstructions are retained, where the attractor reconstructions are ranked according to the mean square error between the power spectra of the reconstructed  $x_1$  variable and of the true  $x_1$  variable over 20000 time steps. The Lyapunov spectra of the trained, autonomous RCs are computed using 100000 time steps. Additionally, the CLE spectra of the driven reservoirs are computed over the 40000 training time steps for these retained reservoirs.

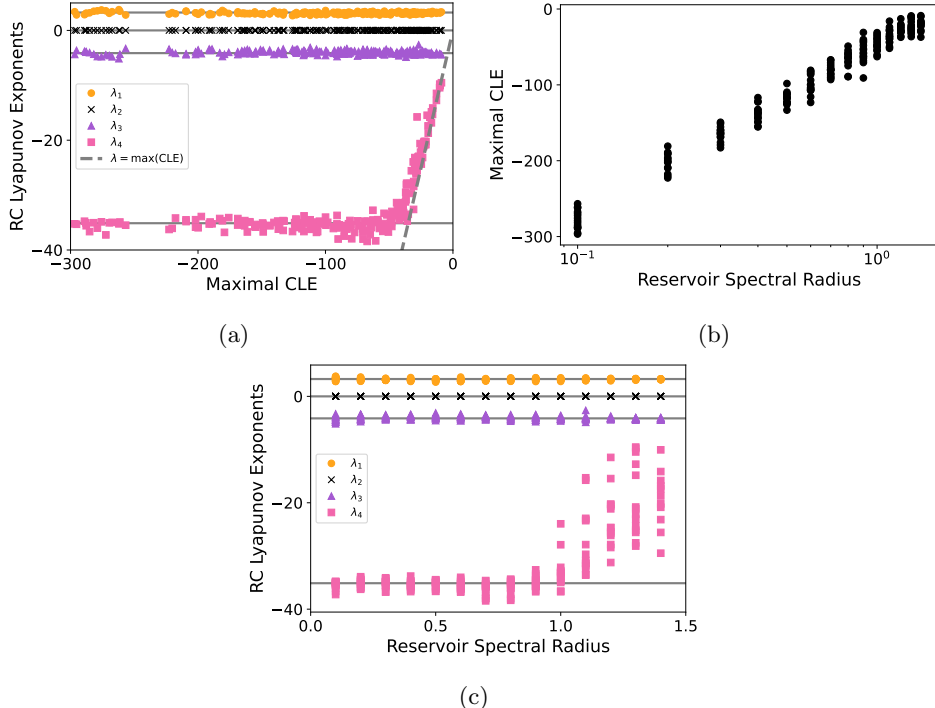


Figure 4: Qi system with  $p_1 = 35$ ,  $p_2 = 10$ ,  $p_3 = 1$  and  $p_4 = 10$ . (a) Three largest Lyapunov exponents of the trained autonomous RC vs the maximal CLE of the driven reservoir before training. The Lyapunov exponents of the true system are indicated as solid gray lines. The line  $\lambda = \max(\text{CLE})$  is shown as a dashed gray line. (b) Maximal CLE of the driven reservoir vs the reservoir spectral radius. (c) Three largest Lyapunov exponents of the trained autonomous RC vs the reservoir spectral radius.

The results of the RC trained on the Qi system are shown in Fig. 4. Figure 4(a) shows the three largest Lyapunov exponents of the autonomous RC plotted as a function of the maximal CLE of the driven reservoir. The Lyapunov exponents of the true Lorenz system are shown as horizontal gray lines. The agreement between the first three Lyapunov exponents of the autonomous RC and the true system Lyapunov exponents is excellent in all cases. For the fourth Lyapunov exponent (pink squares), the agreement is excellent for very negative maximal CLEs. However, as the maximal CLE increases, the disagreement increases significantly. The reason for this disagreement is described in Section 2.2: Once the reservoir CLEs have increased such that they are greater than the most negative LE of the true system, the reservoir dynamics are now too slow to capture the negative LE of the true system, and the maximal CLE of the reservoir replaces the negative LE of the true system as the fourth-largest LE of the autonomous RC. Evidence for this is provided by the fact that the  $\lambda_4$  mostly lie along the curve  $\lambda = \max(\lambda_4^{(Qi)}, \max(\text{CLE}))$ , as predicted in Section 2.2. Again, there appear to be no deleterious effects of having a very negative maximal CLE, corresponding to a short reservoir memory, for this task.

Figure 4(b) shows that the maximal CLE is strongly correlated with spectral radius. Variations for a fixed spectral radius are due to the different input strengths and reservoir network topologies. For confirmation, Fig. 4(c) shows the reservoir Lyapunov exponents as a function of the reservoir spectral radius; one sees that the Lyapunov exponent estimation becomes unreliable for spectral radii greater than about 0.9. The large spread in  $\lambda_4$  for larger values of spectral radius is due to the fact that, at these values of spectral radius,  $\lambda_4$  is determined by the maximal CLE and the maximal CLE is not fully determined by (only strongly correlated with) the spectral radius.

We now consider the effect of the maximal CLE (or the reservoir spectral radius) on the Kaplan-Yorke dimension, shown in Fig. 5. As the maximal CLE nears and surpasses the most negative Lyapunov exponent of the Qi system, the reservoir Kaplan-Yorke dimension does not change. This is expected, because the Kaplan-Yorke dimension of this system depends only on the first three Lyapunov exponents. Therefore, in this case a large reservoir spectral radius (large reservoir maximal

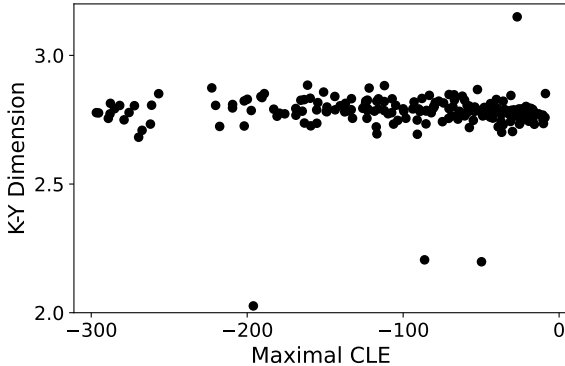


Figure 5: Kaplan-Yorke dimension of the trained autonomous RC vs largest CLE of the driven reservoir before training for the Qi system. For the Qi system, the Kaplan-Yorke dimension of the RC does not depend much on the largest CLE because it is determined solely by the three largest Lyapunov exponents, which are all relatively small in absolute value.

CLE) results in poor estimation of the most negative Lyapunov exponent, but does not impact the dimensionality of the reconstructed attractor.

## 5 Conclusions

We demonstrated that RCs perform best at the attractor reconstruction task when the maximal CLE of the reservoir to the training signal is significantly more negative than the most negative Lyapunov exponent of the true system (or, at least, the most negative Lyapunov exponent that one wishes to reproduce). Attractor reconstruction is defined here as replicating the ergodic properties—here exemplified by the Lyapunov spectra and information dimension—of the true dynamical system [8, 12]. We showed how this is related to the idea that a filter driven by a chaotic system can show an increased fractal dimension if the filter’s CLE is larger than the negative drive system exponents [15]. We also found that the maximal CLE of the reservoir is strongly correlated with the spectral radius of the reservoir.

Our results show how the generalized synchronization behavior of the driven reservoir plays a key role in determining the dynamical behavior of the autonomous RC. While the link between generalized synchronization and reservoir computing has long been understood, we show a quantitative relationship between the rate at which an untrained reservoir approaches generalized synchronization and the performance of the trained RC at the attractor reconstruction task.

Practically, our results can assist the practitioner of reservoir computing. First, our findings suggest that often a RC with a spectral radius significantly smaller than unity performs best at the attractor reconstruction task. Second, when attempting to use reservoir computing to estimate the Lyapunov exponents of an unknown dynamical system, one should compute not only the Lyapunov exponents of the autonomous RC, but also the maximal CLE of the reservoir driven by the training signal. One should only trust the negative Lyapunov exponents from the autonomous RC that are significantly larger than the maximal CLE of the driven reservoir. This is a relatively inexpensive check, since only the maximal CLE must be computed.

Future work includes exploring whether the relationship between the maximal CLE of the driven reservoir and the Lyapunov exponents of the autonomous RC hold in the case where the reservoir is trained only on a single input variable (for example, the Lorenz  $x$  variable only). In this case, the reservoir must create an embedding, and so the reservoir may require some memory to complete this task. As a result, there may be a tradeoff between having enough memory (a large enough maximal CLE) for the embedding and having a small enough maximal CLE for the autonomous RC to reproduce the true negative Lyapunov exponents.

**Acknowledgment** JDH wishes to acknowledge Lou Pecora and Andrew Flynn for insightful discussions.

## References

- [1] Henry Abarbanel. *Analysis of observed chaotic data*. Springer Science & Business Media, 2012.
- [2] Holger Kantz and Thomas Schreiber. *Nonlinear time series analysis*, volume 7. Cambridge University Press, 2004.
- [3] Steven L Brunton and J Nathan Kutz. *Data-driven science and engineering: Machine learning, dynamical systems, and control*. Cambridge University Press, 2022.
- [4] Herbert Jaeger. Tutorial on training recurrent neural networks, covering BPPT, RTRL, EKF and the “echo state network” approach. *German National Research Institute for Computer Science (GMD) Report No. 159*, 2002.
- [5] Herbert Jaeger and Harald Haas. Harnessing nonlinearity: Predicting chaotic systems and saving energy in wireless communication. *Science*, 304(5667):78–80, 2004.
- [6] Jaideep Pathak, Zhixin Lu, Brian R Hunt, Michelle Girvan, and Edward Ott. Using machine learning to replicate chaotic attractors and calculate lyapunov exponents from data. *Chaos*, 27(12), 2017.
- [7] Miki U Kobayashi, Kengo Nakai, Yoshitaka Saiki, and Natsuki Tsutsumi. Dynamical system analysis of a data-driven model constructed by reservoir computing. *Phys. Rev. E*, 104(4):044215, 2021.
- [8] Jason A Platt, Adrian Wong, Randall Clark, Stephen G Penny, and Henry DI Abarbanel. Robust forecasting using predictive generalized synchronization in reservoir computing. *Chaos*, 31(12), 2021.
- [9] J-P Eckmann and David Ruelle. Ergodic theory of chaos and strange attractors. *Rev. Mod. Phys.*, 57(3):617, 1985.
- [10] Masaki Sano and Yasuji Sawada. Measurement of the lyapunov spectrum from a chaotic time series. *Phys. Rev. Lett.*, 55(10):1082, 1985.
- [11] Xubin Zeng, R Eykholt, and RA Pielke. Estimating the lyapunov-exponent spectrum from short time series of low precision. *Phys. Rev. Lett.*, 66(25):3229, 1991.
- [12] Jason A Platt, Stephen G Penny, Timothy A Smith, Tse-Chun Chen, and Henry DI Abarbanel. A systematic exploration of reservoir computing for forecasting complex spatiotemporal dynamics. *Neural Networks*, 153:530–552, 2022.
- [13] Junjie Jiang and Ying-Cheng Lai. Model-free prediction of spatiotemporal dynamical systems with recurrent neural networks: Role of network spectral radius. *Phys. Rev. Research*, 1(3):033056, 2019.
- [14] Andrew Flynn, Vassilios A Tsachouridis, and Andreas Amann. Multifunctionality in a reservoir computer. *Chaos*, 31(1), 2021.
- [15] R Badii, G Broggi, B Derighetti, Ms Ravani, S Ciliberto, A Politi, and MA Rubio. Dimension increase in filtered chaotic signals. *Phys. Rev. Lett.*, 60(11):979, 1988.
- [16] Louis M Pecora and Thomas L Carroll. Discontinuous and nondifferentiable functions and dimension increase induced by filtering chaotic data. *Chaos*, 6(3):432–439, 1996.
- [17] Mantas Lukoševičius and Herbert Jaeger. Reservoir computing approaches to recurrent neural network training. *Computer Sci. Rev.*, 3(3):127–149, 2009.
- [18] Mantas Lukoševičius, Herbert Jaeger, and Benjamin Schrauwen. Reservoir computing trends. *KI-Künstliche Intelligenz*, 26:365–371, 2012.
- [19] Andrei Nikolaevich Tikhonov, AV Goncharsky, Vyacheslav Vasil'evich Stepanov, and Anatoly G Yagola. *Numerical methods for the solution of ill-posed problems*, volume 328. Springer Science & Business Media, 1995.

[20] Daniel J Gauthier, Ingo Fischer, and André Röhm. Learning unseen coexisting attractors. *Chaos*, 32(11), 2022.

[21] Mirko Goldmann, Claudio R Mirasso, Ingo Fischer, and Miguel C Soriano. Learn one size to infer all: Exploiting translational symmetries in delay-dynamical and spatiotemporal systems using scalable neural networks. *Phys. Rev. E*, 106(4):044211, 2022.

[22] Ling-Wei Kong, Yang Weng, Bryan Glaz, Mulugeta Haile, and Ying-Cheng Lai. Reservoir computing as digital twins for nonlinear dynamical systems. *Chaos*, 33(3), 2023.

[23] Dhruvit Patel and Edward Ott. Using machine learning to anticipate tipping points and extrapolate to post-tipping dynamics of non-stationary dynamical systems. *Chaos*, 33(2), 2023.

[24] Amitava Banerjee, Jaideep Pathak, Rajarshi Roy, Juan G Restrepo, and Edward Ott. Using machine learning to assess short term causal dependence and infer network links. *Chaos*, 29(12), 2019.

[25] Amitava Banerjee, Joseph D Hart, Rajarshi Roy, and Edward Ott. Machine learning link inference of noisy delay-coupled networks with optoelectronic experimental tests. *Phys. Rev. X*, 11(3):031014, 2021.

[26] Amirhossein Nazerian, Chad Nathe, Joseph D Hart, and Francesco Sorrentino. Synchronizing chaos using reservoir computing. *Chaos*, 33:103121, 2023.

[27] Piotr Antonik, Marvyn Gulina, Jaël Pauwels, and Serge Massar. Using a reservoir computer to learn chaotic attractors, with applications to chaos synchronization and cryptography. *Phys. Rev. E*, 98(1):012215, 2018.

[28] Daniel Canaday, Andrew Pomerance, and Daniel J Gauthier. Model-free control of dynamical systems with deep reservoir computing. *Journal of Physics: Complexity*, 2(3):035025, 2021.

[29] Jaideep Pathak, Brian Hunt, Michelle Girvan, Zhixin Lu, and Edward Ott. Model-free prediction of large spatiotemporally chaotic systems from data: A reservoir computing approach. *Phys. Rev. Lett.*, 120(2):024102, 2018.

[30] Kengo Nakai and Yoshitaka Saiki. Machine-learning inference of fluid variables from data using reservoir computing. *Phys. Rev. E*, 98(2):023111, 2018.

[31] Troy Arcomano, Istvan Szunyogh, Alexander Wikner, Brian R Hunt, and Edward Ott. A hybrid atmospheric model incorporating machine learning can capture dynamical processes not captured by its physics-based component. *Geophys. Res. Lett.*, 50(8):e2022GL102649, 2023.

[32] Tamaki Suematsu, Kengo Nakai, Tsuyoshi Yoneda, Daisuke Takasuka, Takuya Jinno, Yoshitaka Saiki, and Hiroaki Miura. Machine learning prediction of the MJO extends beyond one month. *arXiv preprint arXiv:2301.01254*, 2022.

[33] Braden Thorne, Thomas Jüngling, Michael Small, Débora Corrêa, and Ayham Zaitouny. Reservoir time series analysis: Using the response of complex dynamical systems as a universal indicator of change. *Chaos*, 32(3), 2022.

[34] Amitava Banerjee, Sarthak Chandra, and Edward Ott. Network inference from short, noisy, low time-resolution, partial measurements: Application to *C. elegans* neuronal calcium dynamics. *Proceedings of the National Academy of Sciences*, 120(12):e2216030120, 2023.

[35] Zhixin Lu, Brian R Hunt, and Edward Ott. Attractor reconstruction by machine learning. *Chaos*, 28(6), 2018.

[36] Nikolai F Rulkov, Mikhail M Sushchik, Lev S Tsimring, and Henry DI Abarbanel. Generalized synchronization of chaos in directionally coupled chaotic systems. *Phys. Rev. E*, 51(2):980, 1995.

[37] Ljupco Kocarev and Ulrich Parlitz. Generalized synchronization, predictability, and equivalence of unidirectionally coupled dynamical systems. *Phys. Rev. Lett.*, 76(11):1816, 1996.

[38] Henry DI Abarbanel, Nikolai F Rulkov, and Mikhail M Sushchik. Generalized synchronization of chaos: The auxiliary system approach. *Phys. Rev. E*, 53(5):4528, 1996.

[39] Louis M Pecora and Thomas L Carroll. Driving systems with chaotic signals. *Phys. Rev. A*, 44(4):2374, 1991.

[40] Atsushi Uchida, Ryan McAllister, and Rajarshi Roy. Consistency of nonlinear system response to complex drive signals. *Phys. Rev. Lett.*, 93(24):244102, 2004.

[41] Thomas Lymburn, David M Walker, Michael Small, and Thomas Jüngling. The reservoir's perspective on generalized synchronization. *Chaos*, 29(9), 2019.

[42] Allen Hart, James Hook, and Jonathan Dawes. Embedding and approximation theorems for echo state networks. *Neural Networks*, 128:234–247, 2020.

[43] Viktoras Pyragas and Kestutis Pyragas. Using reservoir computer to predict and prevent extreme events. *Phys. Lett. A*, 384(24):126591, 2020.

[44] Lyudmila Grigoryeva, Allen Hart, and Juan-Pablo Ortega. Chaos on compact manifolds: Differentiable synchronizations beyond the takens theorem. *Phys. Rev. E*, 103(6):062204, 2021.

[45] Laurent Larger, Miguel C Soriano, Daniel Brunner, Lennert Appeltant, Jose M Gutiérrez, Luis Pesquera, Claudio R Mirasso, and Ingo Fischer. Photonic information processing beyond turing: an optoelectronic implementation of reservoir computing. *Opt. Express*, 20(3):3241–3249, 2012.

[46] Joma Nakayama, Kazutaka Kanno, and Atsushi Uchida. Laser dynamical reservoir computing with consistency: an approach of a chaos mask signal. *Opt. Express*, 24(8):8679–8692, 2016.

[47] Thomas Lymburn, Alexander Khor, Thomas Stemler, Débora C Corrêa, Michael Small, and Thomas Jüngling. Consistency in echo-state networks. *Chaos*, 29(2), 2019.

[48] JL Kaplan and JA Yorke. Functional differential equations and approximation of fixed points. *Lecture notes in mathematics*, 730:204–227, 1979.

[49] Thomas L Carroll. Dimension of reservoir computers. *Chaos*, 30(1), 2020.

[50] Andrew Flynn, Vassilios A Tsachouridis, and Andreas Amann. Seeing double with a multifunctional reservoir computer. *arXiv preprint arXiv:2305.05799*, 2023.

[51] David Verstraeten and Benjamin Schrauwen. On the quantification of dynamics in reservoir computing. In *International Conference on Artificial Neural Networks*, pages 985–994. Springer, 2009.

[52] Joseph D Hart. Estimating the master stability function from the time series of one oscillator via reservoir computing. *Phys. Rev. E*, 108(3):L032201, 2023.

[53] Edward N Lorenz. Deterministic nonperiodic flow. *J. Atmos. Sci.*, 20(2):130–141, 1963.

[54] William Robert Story. *Application of Lyapunov exponents to strange attractors and intact & damaged ship stability*. PhD thesis, Virginia Tech, 2009.

[55] André Röhm, Daniel J Gauthier, and Ingo Fischer. Model-free inference of unseen attractors: Reconstructing phase space features from a single noisy trajectory using reservoir computing. *Chaos*, 31(10), 2021.

[56] Rebecca L Honeycutt. Stochastic Runge-Kutta algorithms. i. white noise. *Phys. Rev. A*, 45(2):600, 1992.

[57] Chris M Bishop. Training with noise is equivalent to tikhonov regularization. *Neural Comput.*, 7(1):108–116, 1995.

[58] Alexander Wikner, Joseph Harvey, Michelle Girvan, Brian R. Hunt, Andrew Pomerance, Thomas Antonsen, and Edward Ott. Stabilizing machine learning prediction of dynamics: Novel noise-inspired regularization tested with reservoir computing. *Neural Networks*, 170:94–110, 2024.

[59] Guoyuan Qi, Shengzhi Du, Guanrong Chen, Zengqiang Chen, and Zhuzhi Yuan. On a four-dimensional chaotic system. *Chaos, Solitons & Fractals*, 23(5):1671–1682, 2005.